ISSN: 2476-6909; Modares. Mech. Eng. *2026;26(12):989-998.*

Modares Mechanical Engineering

DOI: 10.48311/mme.2026.120241.83010
journal homepage: mme.modares.ac.ir

Biomechanical Effects of Different Fillers on Bone Defect Reconstruction: A Comparative Finite Element Analysis

Marjan Pourgholami[1], Farzaneh Safshekan[1*], Ahmad Bagheri[2], Azadeh Ghouchani[3]

[1] Department of Mechanical Engineering, Ahrar Institute of Technology and Higher Education, Rasht, Iran
[2] Department of Mechanical Engineering, University of Gulian, Rasht, Iran
[3] Department of Biomedical Engineering, Faculty of Engineering, University of Isfahan, Isfahan, Iran

ARTICLE INFO

Article Type
Original Research

Article History
Received: May 13, 2026
Revised: August 01, 2026
Accepted: August 16, 2026
ePublished: September 17, 2026

ABSTRACT

Benign bone tumors occur mainly in the epi-metaphyseal region of long bones, and surgery is the most effective treatment. Tumor recurrence and fractures are complications of following surgery. To reduce the risk of these complications, preoperative surgical simulation is recommended. This study uses FEA to investigate the mechanical effect of reconstructed models with different fillers. The simulations are considered for two defects of different sizes in the medial femoral condyle. The small defect simulates tumor curettage and the large defect simulates tumor curettage with some border texture. The fillers include several polymers, ceramics, and bioglasses. The mechanical performance of each filler in the reconstruction of defects under single-leg standing loading is evaluated by examining the maximum principal and von Mises stresses compared to the healthy model. In the epi-metaphyseal region of the healthy model, the maximum principal stress was 5.15 MPa and the maximum von Mises stress was 7.63 MPa. Among the materials tested, polyether ether ketone (PEEK) exhibits stress values very close to healthy bone. (with the values of the principal and von Mises stresses was 5.14 MPa and 7.66 MPa in the small defect and 5.16 MPa and 7.7 MPa in the large defect, respectively). However, Hydroxyapatite (HA), Beta-tricalcium phosphate and bioglasses showed the least mechanical compliance, which increased with increasing defect size. Comparison of the results obtained shows that the choice of filler depends on the size of the defect. These findings highlight the role of FEA in predicting surgical outcomes and postoperative bone strength.

Keywords: Finite Element Analysis, Femur, Filler, Bone Tumor

How to cite this article
Pourgholami M, Safshekan F, Bagheri A, Ghouchani A, Biomechanical Effects of Different Fillers on Bone Defect Reconstruction: A Comparative Finite Element Analysis. Modares Mechanical Engineering; *2026;26(12):989-998.*

*Corresponding author's email: f.safshekan@ahrar.ac.ir
*Corresponding ORCID ID: 0000-0002-9170-3662

شاپا: ۲۴۷۶-۶۹۰۹؛ مهندسی مکانیک مدرس. ۹۹۸-۹۸۹:(۱۲)۱۴۰۵;۲۶

مهندسی مکانیک مدرس

DOI: 10.48311/mme.2026.120241.83010

صفحه اصلی مجله: mme.modares.ac.ir

تأثیر بیومکانیکی پرکننده های مختلف بر بازسازی نقص استخوانی پس از کورتاژ: تحلیل تطبیقی اجزای محدود

مرجان پورغلامی[۱]، فرزانه صفشکن[۱*]، احمد باقری[۲] ، آزاده قوچانی[۳]

[۱] گروه مهندسی مکانیک، مؤسسه آموزش عالی احرار، رشت، ایران

[۲] دانشکده مهندسی مکانیک، دانشگاه گیلان، رشت، ایران

[۳] گروه مهندسی پزشکی، دانشکده مهندسی، دانشگاه اصفهان، اصفهان، ایران

اطلاعات مقاله

نوع مقاله

مقاله پژوهشی

تاریخچه مقاله

دریافت: ۱۴۰۵/۰۲/۲۳

بازنگری: ۱۴۰۵/۰۵/۱۰

پذیرش: ۱۴۰۵/۰۵/۲۵

ارائه آنلاین: ۱۴۰۵/۰۶/۲۶

چکیده

تومورهای خوش‌خیم استخوانی عمدتاً در ناحیه اپی متافیز استخوان‌های بلند رخ می‌دهند و جراحی مؤثرترین درمان است. عود تومور و شکستگی از عوارض این جراحی هستند. برای کاهش خطر این عوارض، شبیه‌سازی جراحی قبل از عمل توصیه می‌شود. این مطالعه با استفاده از آنالیز المان محدود، تاثیر مکانیکی مدل‌های بازسازی‌شده با پرکننده‌های مختلف را بررسی می‌کند. شبیه‌سازی‌ها برای دو نقص با اندازه‌های مختلف در کندیل داخلی استخوان ران در نظر گرفته شده است. نقص کوچک‌تر فقط کورتاژ تومور و نقص بزرگ‌تر کورتاژ تومور به همراه مقداری بافت حاشیه‌ی آن را شبیه‌سازی میکنند. پرکننده‌ها شامل پلیمرها، سرامیک‌ها و بیوگلاس هستند. عملکرد مکانیکی هر پرکننده در بازسازی مدل‌ها تحت بارگذاری ایستاده روی یک پا با بررسی حداکثر تنش‌های اصلی و فون میزس در مقایسه با مدل سالم ارزیابی می‌شود. در ناحیه اپی متافیز مدل سالم، حداکثر تنش اصلی ۵/۱۵ مگاپاسکال و حداکثر تنش فون میزس 7.63 مگاپاسکال بود. در میان مواد آزمایش‌شده، پلی‌اتر اتر کتون (PEEK) مقادیر تنش بسیار نزدیکی به استخوان سالم نشان می‌دهد (با مقادیر تنش‌های اصلی و فون میزس که به ترتیب ۵.۱۴ مگاپاسکال و ۷.۶۶ مگاپاسکال در نقص کوچک و ۵.۱۶ مگاپاسکال و ۷.۷ مگاپاسکال در نقص بزرگ). اما هیدروکسی آپاتیت(HA)، بتاتری کلسیم فسفات و شیشه‌های زیستی کمترین تطابق مکانیکی را نشان دادند که با افزایش اندازه نقص، شدت یافت. مقایسه نتایج به دست آمده نشان می‌دهد که انتخاب نوع پرکننده به اندازه نقص بستگی دارد. این یافته‌ها نقش FEA را در پیش‌بینی نتایج جراحی و استحکام استخوان پس از عمل برجسته می‌کند.

کلیدواژه‌ها: تحلیل اجزای محدود، استخوان ران، پرکننده، تومور استخوانی

نحوه ارجاع به این مقاله

پورغلامی مرجان، صفشکن فرزانه، باقری احمد، قوچانی آزاده، تأثیر بیومکانیکی پرکننده های مختلف بر بازسازی نقص استخوانی پس از کورتاژ: تحلیل تطبیقی اجزای محدود ، مهندسی مکانیک مدرس. ۹۹۸-۹۸۹:(۱۲)۱۴۰۵;۲۶

*پست الکترونیکی نویسنده عهده‌دار مکاتبات: f.safshekan@ahrar.ac.ir

*شناسه ارکید نویسنده عهده‌دار مکاتبات: 0000-0002-9170-3662

1- Introduction

Benign bone tumors (BBTs), which are composed of various neoplasms, account for 40–50% of all bone tumors. Types of these tumors include giant cell tumor and aneurysmal bone cyst[1,2]. BBTs can occur in any skeletal region[3]; however, they most commonly appear around the knee joint[4]. The most effective treatment for BBTs is surgery, especially for large and aggressive tumors that weaken the bone and cause pathological fractures[5]. This surgery is performed in two stages. In the first stage, the tumor is cured, and in the second stage, the defect created by the curettage is reconstructed. Reconstruction is often performed using synthetic fillers such as polymethyl methacrylate polymers or hydroxyapatite ceramics[6]. Although surgery is the most effective treatment for BBTs, it also has complications. For example, tumor recurrence, which affects about half of the patients who undergo surgery, is one of the most common complications of surgery for this type of tumor[7]. Postoperative fractures, especially at the junction between the filler and the adjacent bone, are another challenge with this treatment method[8]. To reduce the risk of these complications, special attention should be paid to the amount of bone removal and methods of bone defect reconstruction. The optimal degree of curettage is very important. If only the tumor is cured, the risk of tumor recurrence is high; however, excessive curettage of the surrounding tissue can compromise bone strength. Fractures are often caused by inadequate fixation of the filler in the defect and premature loading of the operated bone. Successful reconstruction should take into account the characteristics of the defect, the level of bone quality, and the patient's activity[6]. Many studies emphasize the reconstruction of bone defects using synthetic bone substitutes. According to these studies, although autografts are biologically suitable for defect reconstruction, their use is rarely performed due to limited access and donor site complications[9,10]. A study was conducted in 2023 reviewed dual-purpose bone substitutes for the treatment of bone defects after bone tumor resection. The study examined composites that, in addition to defect repair, also exert local anticancer effects via drug release or hyperthermia. The results of this review highlight the dual functionality of these composites but emphasize the need for further validation in clinical settings[11]. A 2024 study of calcium sulfate-calcium phosphate grafts as defect fillers following curettage of benign tumors of the lower extremities was conducted. The results of this study showed that the use of calcium sulfate-calcium phosphate grafts resulted in a faster return to full weight-bearing capacity (mean 6 weeks) and was therefore recommended as a suitable filler compared to autograft grafts. However, this study provided limited data on mechanical compliance in larger defects[12]. Another study was conducted in 2025 on the management of bone tumors, advances in bone grafting techniques, and bone substitutes. This study discussed fillers such as bioactive glasses and calcium sulfate-phosphate composites for post-curettage defects. It also highlighted the lack of comparative biomechanical evaluations, particularly in specific areas such as the femur[13].

Analytical methods such as finite element analysis (FEA), as a biomechanical approach, are an important tool for conducting efficient studies and simulations in this field[8]. For example, Aroonjarattham et al., in a study based on finite element simulation, compared two widely used materials in bone defect reconstruction (PMMA and HA) and found HA to be suitable based on the distribution of von Mises stress and total strain[14]. In a 2019 study using FEA, Dou et al. emphasized the need for reconstruction of large bone defects. Their results from finite element analysis of the proximal femur showed that failure to reconstruct the defect caused by curettage of a bone tumor can increase stress concentration by up to 33%. This increased stress concentration increases the risk of fracture in the bone[15].

Wu et al. (2022) also used the finite element method to find that in order to use bone grafts such as autografts or synthetic fillers to reconstruct large bone defects, these materials must be placed inside a scaffold that conforms to the defect geometry to provide sufficient strength to support the filler[16]. However, there is a gap in the comparison between fillers, including polymers, ceramics, and bioglasses in the same patient condition.

To address this gap, the present study aims to compare the biomechanical performance of several common synthetic fillers, including polymers, bioglasses, and ceramics, in reconstructing femoral bone defects following tumor curettage, using finite element analysis based on CT images. The mechanical behavior of each reconstructed model is evaluated against the intact healthy femur, with maximum principal stress and von Mises stress in the epi-metaphyseal region serving as reference criteria. Additionally, the effect of defect size on the mechanical performance of each filler is systematically investigated. By providing a comparative biomechanical assessment across different filler types and defect sizes, this study offers a preliminary, preoperative method to guide the selection of the most appropriate filler, ultimately contributing to optimized surgical outcomes and reduced postoperative complications.

2- Materials and Methods

2-1- Geometry of the model

2D data obtained from a CT scan of a healthy femur of a 30-year-old woman weighing 65 kg were imported into Mimics software (Materialise, Belgium, version 21.1) to generate a 3D model. To allow distinct material properties to be assigned to each tissue type, the cortical and cancellous bones were segmented into separate masks based on Hounsfield unit (HU) thresholding. Following the default CT data set calibration in Mimics software, voxels with values ranging from 226 to 750 HU were assigned to the cancellous bone mask, while voxels in the range of 750 to 3071 HU were assigned to the cortical bone mask, followed by manual slice-by-slice correction to preserve anatomical continuity at the cortical-cancellous boundary and to remove segmentation artifacts. The two masks were then exported separately to 3-Matic (Materialise, Belgium, version 13), where necessary corrections were made and the point cloud models were converted into surface and volume models (Fig. 1A). Finally, the models were imported into Abaqus software (Dassault Systèmes, version 2021) for finite element analysis

Defects in the medial of femoral's condyle were simulated using the Partition tool in the Part module. The smaller defect with a volume of 40.75mm^3 resulted from tumor curettage. A larger defect with a volume of 86.41mm^3 resulted from tumor curettage plus 5–10% of surrounding tissue. The size of these defects was selected based on the study of Ghouchani et al. on simulated GCT on the medial side of the femoral condyle[17]. The location and size of the tumors are shown in Fig. 1B.

2-2- Mechanical Properties of Bone and Materials

Bone tissues are considered linearly elastic and transversely anisotropic in modeling, and their properties are listed in Table 1.

Table 1 Mechanical properties of bone tissues [18].

Bone Type	Young's Moduli (MPa)	Shear Moduli (MPa)	Poisson's Ratio
Cortical	E1= 16000	G12= 3300	V12= 0.30
	E2= 6300	G23= 3600	V23= 0.45
	E3= 6300	G13= 3300	V13= 0.30
Cancellous	E1= 1352	G12= 399	V12= 0.30
	E2= 822	G23= 370	V23= 0.30
	E3= 822	G13= 399	V13= 0.30

The defects were then reconstructed with 11 fillers including polymers such as Polymethyl methacrylate (PMMA), Polyether ether ketone (PEEK), Poly-L-lactic acid (PLLA), Poly(lactic-co-glycolic acid) (PLGA) and Calcium phosphate cements such as Hydroxyapatite (HA), Dicalcium phosphate dihydrate (also known as brushite), Apatite, Anhydrous monocalcium phosphate (also known as monetite), Beta-tricalcium phosphate (Beta-TCP), Calcium sulfate (CSC) and Bioactive glasses. The mechanical properties of the fillers were assumed to be homogeneous and isotropic (Table 2).

Table 2 Mechanical properties of filler materials

Materials	Young's modulus (MPa)	Poisson's ratio	Reference
PMMA	1800	0.35	[14]
PEEK	3600	0.38	[19]
PLLA	2800	0.38	[20]
PLGA	1400	0.38	[21]
HA	40000	0.27	[14]
Brushite	24300	0.26	[22]
Apatite	13500	0.21	[22]
Monetite	7100	0.20	[22]
Beta-TCP	33100	0.30	[23]
CSC	800	0.30	[24]
Bioglasses	35000	0.27	[25]

2-3- Meshing

The model was meshed using second-order C3D10 tetrahedral elements. A mesh sensitivity analysis was performed to determine the optimal element size, evaluating four progressively refined mesh densities consisting of approximately 17,500, 35,000, 70,000, and 140,000 elements. For each density, the maximum principal stress within the epi-metaphyseal region (the primary region of interest) was recorded as the convergence criterion. The variation between successive refinement levels is presented in Figure 2. Critically, the difference between the 70,000- and 140,000-element meshes was less than 1%, indicating that the solution had effectively converged at the 70,348-element level. Accordingly, this mesh density (100676 nodes) was selected for all subsequent simulations, as further refinement yielded negligible improvements in accuracy.

2-4- Boundary conditions and loading

All femoral models were fixed in all directions. Loading was simulated in standing position on one leg. In this type of loading, a vertical force equal to the person's weight (650 N) is applied to the femoral head (Fig. 1C) [26]. To assess the sensitivity of our results to the applied load magnitude, we performed an additional analysis on the intact model under four load levels: 520 N (80% of reference), 650 N (reference), 780 N (120% of reference), and 850 N (~130% of reference). This range was selected to encompass physiological variations in body weight distribution during single-leg stance, as well as mild dynamic overloads that may occur during daily activities. For each load level, the maximum principal stress in the epi-metaphyseal region was recorded to evaluate the model's response across the tested range. Additionally, the maximum force residual was extracted from Abaqus Job Diagnostics for each load level to verify numerical convergence.

The outputs of the simulation are the maximum principal stress (failure criterion) and the von Mises stress (yield criterion) [27]. The stress distribution analysis was focused on the epi-metaphyseal region of the bone (Figure 1D).

2-5- Computational Specifications

All simulations were performed as static, linear elastic analyses using the Abaqus/Standard implicit solver. A single static load step was applied for each model, consistent with the linear elastic assumption for the materials. The simulations were executed using Abaqus 2021 on a laptop with an Intel Core i7-7500U CPU @ 2.70GHz and 8.00 GB RAM, running a 64-bit operating system. The average solution time was approximately 2 minutes per simulation.

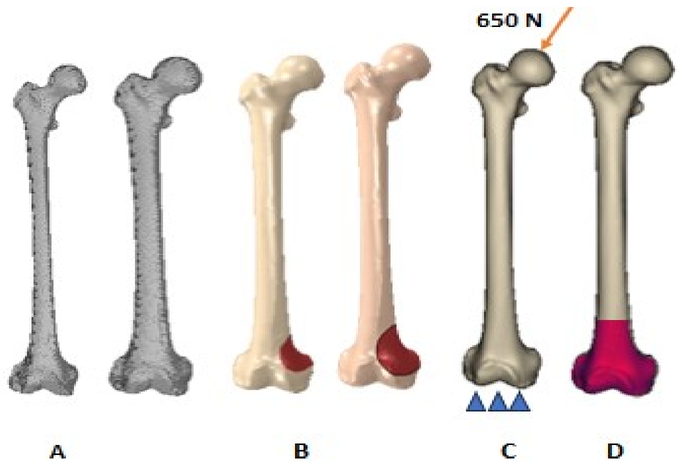

Fig.1 (A) Masks of cortical and cancellous tissues. (B) Tumor locations and sizes. (C) Boundary conditions and loading.(D) Region of investigation highlighted in red.

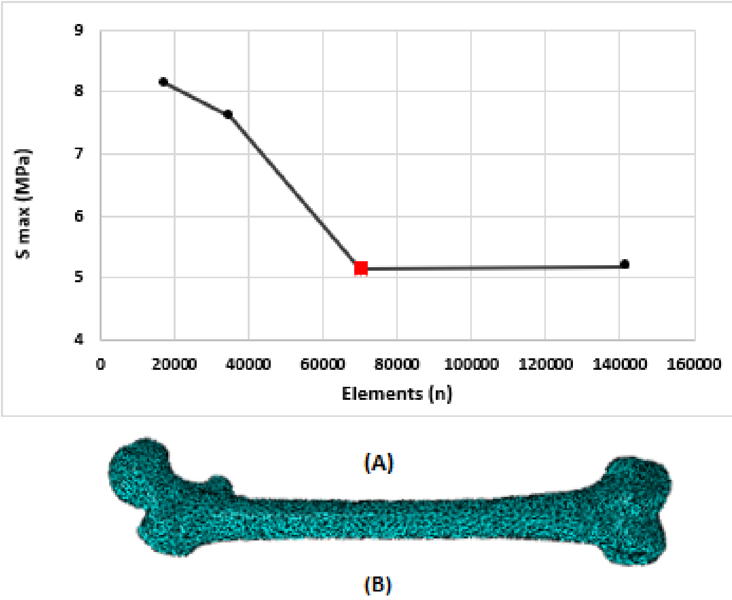

Fig.2 Mesh convergence analysis. (A) Maximum principal stress in the epi-metaphyseal region as a function of element number. (B) Final meshed model with the selected 70348-element density.

2-6- Model Validation

Model validation was performed by comparing our predicted maximum von Mises stress with the results reported by Yang et al. (2010) [28], who employed a full femur geometry under similar loading conditions (500 N, neutral alignment). The maximum von Mises stress in their orthotropic inhomogeneous model (M1, 7,934 elements) was reported to be 35.9 MPa, while in our model, this parameter was predicted to be 30.75 MPa, indicating a 14.3% difference.This discrepancy arises from several factors, including assignment of differnet material properties (inhomogeneous versus homogeneous properties, although both studies use orthotropic properties), and also differences in mesh refinement (7,934 vs. 70,000 elements), location of stress measurement (distal diaphysis vs. epi-metaphyseal region), and patient-specific geometric features in their work and the present study. Nevertheless, this difference falls within acceptable validation ranges reported in the literature, with deviations of 10–20% considered acceptable for femoral FEA validation[29][30]. Therefore, our model demonstrates sufficient agreement with the reference study, which validates its predictive capability."

3- Results

To evaluate sensitivity to load magnitude, the maximum principal stress in the epi-metaphyseal region was recorded at 520 N, 650 N, 780 N, and 850 N, yielding 4.16, 5.17, 6.18, and 6.7 MPa, respectively. As shown in Figure 3A, the maximum principal stress increased linearly with the applied load ($R^2 > 0.999$), confirming that the model response remains proportional within the tested range. The maximum force residuals for the same load levels are also presented in Figure 3B, ranging from approximately 0.75×10^{-9} N to 1.55×10^{-9} N (roughly eleven orders of magnitude smaller than the applied loads) confirming that global force equilibrium was achieved with very high numerical accuracy across all load levels tested. This linear relationship indicates that the reference load of 650 N is appropriate for the single-leg standing scenario examined in this study and that proportional variations in load magnitude would not affect the relative differences or rank order of stress distributions across the compared models.

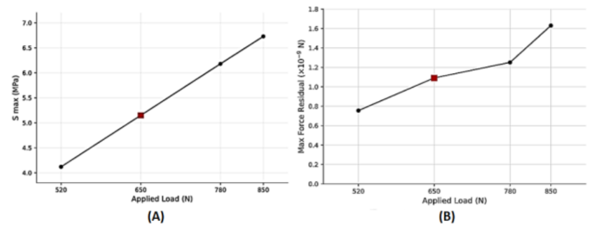

Fig. 3 (A) Loading sensitivity analysis. Maximum principal stress versus applied load, showing a linear relationship ($R^2 > 0.999$). (B) Maximum force residual versus applied load

All models containing reconstructed defects were compared with the intact model under the same loading. The focus of this study was on the distributed stresses in the epi-metaphyseal region. The results of the distribution of the maximum principal stresses on the bone models are shown in Figure 4.

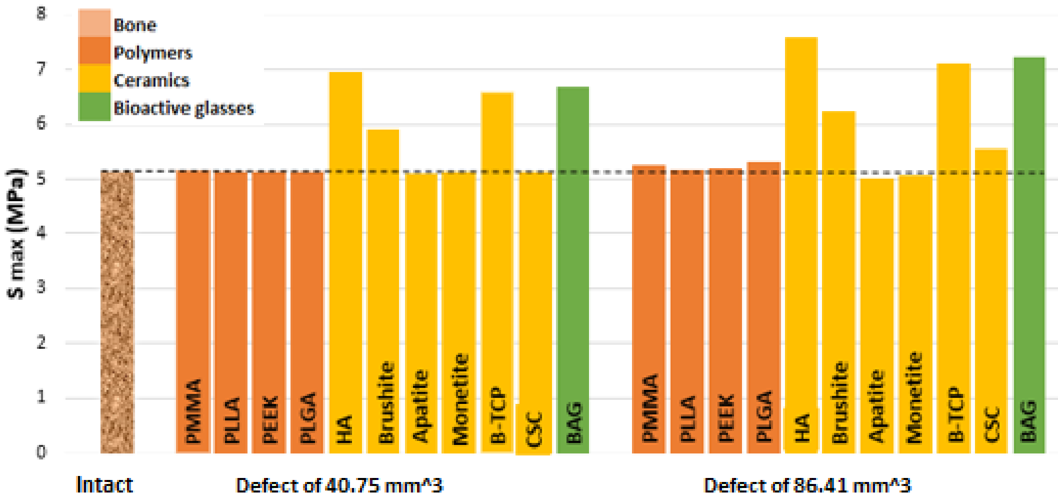

Fig.4 Maximum principal stress (MPa) across intact and reconstructed models.

Maximum principal stress in the intact model is 5.15 MPa (Fig 5A). Most of the reconstructed models with polymeric fillers - especially PEEK and PLLA- showed maximum principal stress values very close to the intact model (4.8-5.5 MPa)(Fig 5B). Increasing the defect size also did not significantly affect the stress distribution on these models. In contrast, models filled with stiffer ceramics such as HA, β-TCP and bioactive glass developed much higher stresses.

They reached 6.57-6.95 MPa in smaller defects and up to 15% higher in larger defects than the stress on the intact model (Fig 5C). This increase indicates a mechanical mismatch and greater load transfer to the host bone. Figure 6 shows the results of the maximum von Mises stress values in the epi-metaphyseal region of the models.

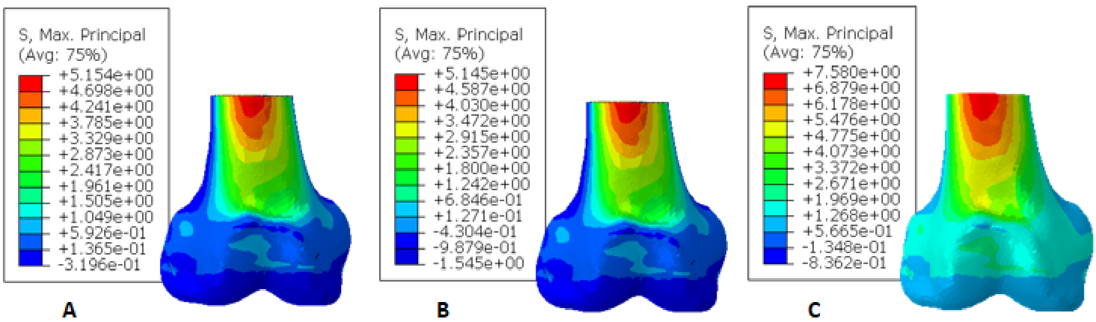

Fig. 5 Maximum principal stress contours: (A) Intact. (B) PEEK-reconstructed. (C) HA-reconstructed.

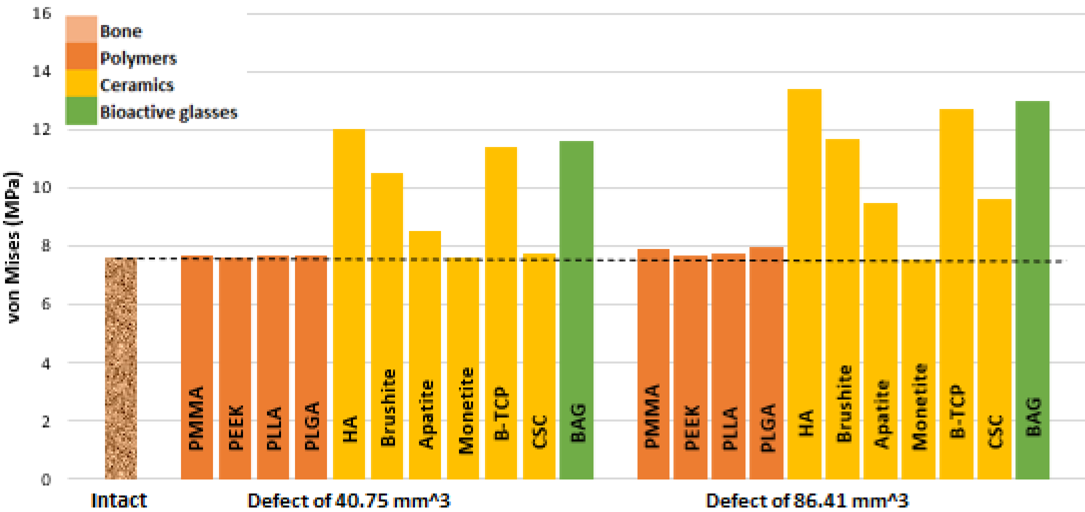

Fig.6 von Mises stress (MPa) across models.

The maximum von Mises stress in intact model is 7.63 MPa.

The models filled with polymer fillers developed a similar stress range to the intact model. The maximum von Mises stress values in these models were in the range of 7.6–8.0 MPa. Increasing the defect size also had no effect on the stress distribution in these models. The models reconstructed with Monetite also had maximum von Mises stress values close to the intact model. And this stress value remained unchanged with increasing defect volume.

The models containing ceramic fillers resulted in much higher stress concentrations, with the HA-repaired model reaching more than 13 MPa, an increase of about 70% compared to intact bone. Larger defects increased the interfacial stresses by 20–30%. The following are images of the distribution of von Mises stress in the intact model (Figure 7A), the model containing a large defect and reconstructed with PEEK (Figure 7B), and the model containing a large defect and reconstructed with HA (Figure 7C).

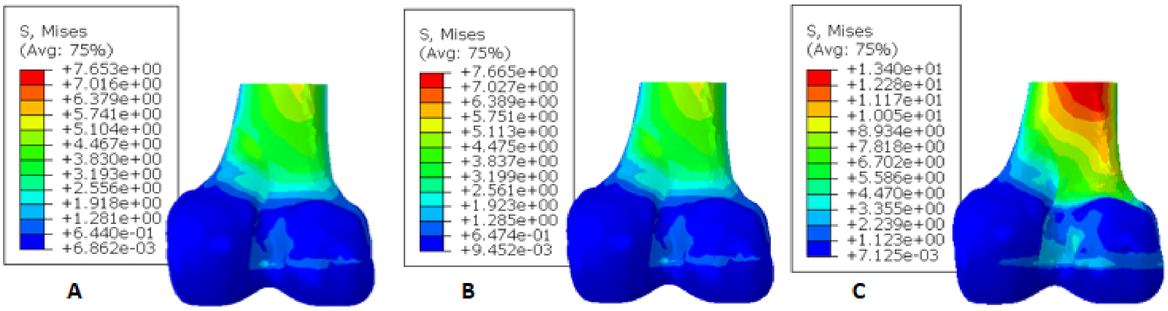

Fig. 7 von Mises stress contours: (A) Intact. (B) PEEK-reconstructed. (C) HA-reconstructed.

4- Discussion

The present study aimed to investigate the biomechanical performance of various synthetic fillers used for the reconstruction of bone defects following curettage of benign bone tumors by means of finite element analysis. By simulating clinically relevant defect sizes under physiological single-leg standing conditions, the mechanical response of reconstructed femoral models was systematically compared with that of an intact femur.

Postoperative complications associated with benign bone tumor surgery—most notably tumor recurrence and secondary fracture—remain a considerable clinical concern. Reported recurrence rates approach 50%[7]), while fractures frequently occur at the bone–filler interface due to mechanical mismatch or premature loading. These complications underscore the importance of optimizing both the extent of curettage and the mechanical compatibility of reconstruction materials, particularly in load-bearing regions such as the epi-metaphyseal of the femur[8].

In the present analysis, stress distributions within the epi-metaphyseal region of the intact femur revealed maximum principal and von Mises stresses of 5.15 MPa and 7.63 MPa, respectively. These values served as a biomechanical benchmark for evaluating reconstructed models. From a mechanical standpoint, an optimal filler should reproduce stress levels comparable to those of healthy bone in order to minimize stress shielding, excessive interfacial loading, and the risk of secondary fracture.

4-1- Biomechanical Evaluation of Polymers

Among the investigated materials, polymer-based fillers demonstrated the most favorable biomechanical performance across both defect sizes. In particular, models reconstructed with PEEK and PLLA exhibited stress distributions that closely approximated those of the intact femur, with minimal sensitivity to increases in defect volume. This behavior can be attributed to the elastic moduli of these polymers, which more closely match that of cortical bone compared to stiffer ceramic materials.

PEEK, with an elastic modulus of approximately 3.6 GPa, has the closest mechanical match to healthy bone. Findings suggest that the resulting uniform stress transfer reduces stress concentration in the host tissue and the risk of bone fracture under loading even within 2–4 weeks after surgery [21,31,32]. These findings are consistent with the results of Zhang's study in 2025. According to his study, PEEK-based implants and scaffolds allow for early weight-bearing while maintaining structural stability [33]; However, the limited bioactivity and biodegradability of PEEK may limit long-term bone ingrowth, suggesting that surface modification or bioactive coatings may be necessary to enhance osseointegration[31].

Poly-L-lactic acid (PLLA) is a biodegradable and biocompatible material that is widely used in bone repair. It is degraded in the body over a relatively short period of time (6–12 months) and replaced by new tissue. PLLA supports cell growth and reduces pressure on the new bone, helping to promote healing[34,35]. Clinical trials report >80% union in non-load-bearing defects[36], and PLLA/CaP composite scaffolds promote new bone formation after 6 months[37], but brittleness in high-load areas increases the risk of fracture under cyclic loading[38].

PMMA provided immediate mechanical stability and remains widely used due to its ease of application and tumoricidal thermal effects[39]. Despite these advantages, slightly elevated stresses were observed in larger defects, which may contribute to cartilage degeneration and long-term joint complications[40]. Consequently, while PMMA remains effective for short-term stabilization, its mechanical and thermal limitations warrant cautious use near articular surfaces[41].

4-2- Biomechanical Evaluation of Ceramics

Ceramic-based fillers exhibited a markedly different mechanical response compared to polymeric materials. Monetite was the only ceramic filler that generated stress levels comparable to those of intact bone[22,39]. Its rapid absorption into the body and high biocompatibility facilitate bone regeneration. However, its brittle nature, high cost, and time-consuming synthesis limit its use, especially in high-load applications[37,42].

In contrast, ceramics such as hydroxyapatite and β-tricalcium phosphate, due to their greater stiffness compared to bone, resulted in the concentration of principal and von Mises stresses at the bone-filler interface. These stress values increased with increasing defect size, indicating a greater likelihood of stress shielding and interface failure. While these materials offer excellent bone conduction, their mechanical mismatch with the host bone represents a significant limitation in their use in load-bearing areas[14,31]

4-3- Biomechanical Evaluation of Bioactive glasses

Bioactive glass fillers generated higher stress levels relative to polymer-based reconstructions, reflecting their high stiffness. Despite this mechanical drawback, bioactive glasses possess superior biological properties, including angiogenesis promotion and enhanced osteogenic response[25,43], Consequently, their application may be advantageous in small or non-load-bearing defects, where biological performance outweighs mechanical demands. In load-bearing scenarios, however, their brittleness and elevated stress concentrations may increase fracture risk[32].

4-4- Clinical Implications

The present findings emphasize that no single filler material is universally optimal for all clinical scenarios. Instead, filler selection should be tailored to patient-specific factors, including defect size, bone quality, activity level, and postoperative loading expectations[6,7]. Younger and more active patients may benefit from polymer-based fillers such as PEEK or PLLA, which provide favorable mechanical compatibility and reduced fracture risk[21,44,45], Conversely, in older patients or in cases involving smaller defects with controlled loading, bioactive ceramics may be clinically acceptable despite their higher stiffness[14,46].

This patient-specific approach supports a departure from a "one-size-fits-all" reconstruction strategy and highlights the role of finite element analysis as a preoperative planning tool. By predicting mechanical outcomes under physiological loading, FEA can assist surgeons in optimizing reconstruction strategies and potentially reducing postoperative complications.

4-5- Limitations and Future Directions

Several limitations of the present study should be acknowledged. All materials were modeled as linearly elastic, and the time-dependent degradation of biodegradable fillers as well as bone remodeling were not considered. Furthermore, loading conditions were limited to static single-leg standing, whereas daily activities such as walking, stair climbing, and rotational movements impose complex dynamic loads. Additionally, the analysis was performed on a single femoral geometry, which limits the generalizability of the findings; however, this approach was intentionally chosen to isolate and compare the effect of filler material on biomechanical performance while controlling for inter-subject geometric variability. This methodology is consistent with established FEA practice in orthopedic biomechanics, where a representative anatomical model is commonly used for controlled parametric comparisons of implants, fixation methods, and scaffolds[17,47,48].

Future studies should incorporate additional patient-specific geometries differing in age, sex, and bone quality, cyclic and multi-directional loading scenarios, and experimental or in vivo validation to assess long-term mechanical performance and fatigue behavior. Furthermore, if finite element analysis is performed based on Quantitative Computer Tomography (QCT) images, it is possible to assign heterogeneous mechanical properties of bone. The determination of heterogeneous properties is based on Hounsfield numbers and their numerical relationship with bone density at each point[49,50]. The investigation of composite fillers combining polymeric and ceramic phases may also provide an effective strategy to balance mechanical compatibility and biological functionality.

5- Conclusion

This study presents a systematic biomechanical comparison of a wide range of synthetic fillers (including polymers, ceramics, and bioactive glass) using a single, uniform finite element approach, with all materials evaluated under identical patient-specific conditions and compared against the same healthy bone model. Using a CT-based finite element model with two clinically relevant defect sizes, the mechanical behavior of each filler was assessed relative to intact bone to guide evidence-based surgical decision-making.

The results showed that the finite element model reconstructed with polymers particularly, polyether ether ketone (PEEK) mimicked the mechanical behavior of healthy bone more accurately than any other filler material. In this model, the maximum principal and von Mises stresses were 5.14 MPa and 7.66 MPa, respectively, which are nearly identical to the healthy bone reference values of 5.15 MPa and 7.65 MPa, with a deviation of less than 1% observed at both defect sizes. This close agreement indicates that PEEK provides excellent mechanical compatibility with the host bone. In contrast, the model reconstructed with hydroxyapatite (HA) showed a substantial increase in stress; as von Mises stress increased by approximately 70% and the maximum principal stress by approximately 47% compared to healthy bone, particularly in larger defects. Similarly, Beta-TCP and bioactive glass exhibited elevated stresses, indicating a mechanical mismatch with the host bone and a potential risk of stress shielding.

These findings provide a quantitative basis for preoperative filler selection, demonstrating that PEEK offers superior mechanical compatibility under static loading, particularly for larger defects where stress shielding and fracture risk are primary concerns. However, clinical use requires further studies under dynamic loading and experimental validation, and the final choice should depend on the patient's defect size, bone quality, and functional needs.

Artificial Intelligence Statement: We explicitly state that, during the preparation of this work, artificial intelligence tools were used solely to support the writing and translation processes.

Funding: This research did not receive any specific grant from funding agencies in the public, commercial, or non-profit sectors.

CRediT Authorship Contribution: Marjan Pourgholami: Writing, software (30%). Farzaneh Safshekan: Supervision, overall project design (25%). Ahmad Bagheri: Supervision, data analyst (20%). Azadeh Ghoochani: Review and editing, methodologist, data analyst (25%).

Ethics Approval:

The scientific content of this article is the result of the authors' research and has not been published in any Iranian or international journal.

Conflict of Interest:

There are no other conflicts of interest to declare.

References

[1] D. N. Hakim, T. Pelly, M. Kulendran, and J. A. Caris, "Benign tumours of the bone: A review," *J. Bone Oncol.*, vol. 4, no. 2, pp. 37–41, 2015, doi:10.1016/j.jbo.2015.02.001.

[2] H. Fritzsche, K. D. Schaser, and C. Hofbauer, "Benigne Tumoren und tumorähnliche Läsionen des Knochens: Allgemeine Behandlungsprinzipien," *Orthopade*, vol. 46, no. 6, pp. 484–497, 2017, doi:10.1007/s00132-017-3429-z

[3] H. Sugiyama *et al.*, "Characteristics of Benign and Malignant Bone," *JBJS Open Access*, vol. 3, no. 2, pp. 1–11, 2018.

[4] P. Behrendt, T. Grunow, F. K-H, M. Krause, H. Fahlbusch, and M. Priemel, "Correction to: Not every knee tumour is a ganglion - retrospective analysis of benign and malign tumour entities around the knee (Archives of Orthopaedic and Trauma Surgery, (2024), 10.1007/s00402-024-05401-7)," *Arch. Orthop. Trauma Surg.*, pp. 3227–3234, 2024, doi:10.1007/s00402-024-05494-0.

[5] I. T. Badr, M. M. Moawad, A. O. Elgebery, B. A. Hakim, and B. Z. Hasan, "Filling of the resultant cavity after curettage of benign bone tumours is still controversial," *Med. J. Malaysia*, vol. 78, no. 2, pp. 163–170, 2023.

[6] A. Ghouchani and G. Rouhi, "The Great Need of a Biomechanical-Based Approach for Surgical Methods of Giant Cell Tumor: A Critical Review," *Journal of Medical and Biological*

Engineering, vol. 37, no. 4. Springer Berlin Heidelberg, pp. 454–467, Aug. 01, 2017. doi:10.1007/s40846-017-0278-5.
[7] Y. Wang, Q. Tian, C. Wu, H. Li, J. Li, and Y. Feng, "Management of the Cavity After Removal of Giant Cell Tumor of the Bone," *Front. Surg.*, vol. 8, no. July, pp. 1–13, 2021, doi:10.3389/fsurg.2021.626272.
[8] A. Ghouchani, M. H. Ebrahimzadeh, and G. Rouhi, "The Most Appropriate Reconstruction Method Following Giant Cell Tumor Curettage: A Biomechanical Approach," 2018. [Online]. Available: http://abjs.mums.ac.irtheonlineversionofthisarticleabjs.mums.ac.ir.
[9] R. Morrison, "Bone Grafts and Bone Graft Substitutes," *Man. Spine Surg. Second Ed.*, pp. 77–82, 2023, doi:10.1007/978-3-662-64062-3_12.
[10] J. H. Cho and H. K. Song, "Current concepts and applications of bone graft substitutes in orthopedic surgery," vol. 38, no. 4, pp. 169–177, 2025. doi:10.12671/jmt.2025.00248.
[11] Z. Wang, I. C. van der Geest, S. C. Leeuwenburgh, and J. J. van den Beucken, "Bifunctional bone substitute materials for bone defect treatment after bone tumor resection," *Mater. Today Bio*, vol. 23, no. October, p. 100889, 2023, doi:10.1016/j.mtbio.2023.100889.
[12] L. Gyemi, A. Selznick, B. Petrisor, and M. Ghert, "Time to full weight-bearing with the use of a calcium sulfate-calcium phosphate bone substitute as a bone void filler following extended curettage in the treatment of primary benign bone tumours," *J. Orthop. Surg.*, vol. 32, no. 2, pp. 1–9, 2024, doi:10.1177/10225536241254200.
[13] S. Sakdejayont, T. Chobpenthai, P. Suksirivecharuk, I. F. Ninatkiattikul, and T. Poosiripinyo, "A Review on Bone Tumor Management: Cutting-Edge Strategies in Bone Grafting, Bone Graft Substitute, and Growth Factors for Defect Reconstruction," *Orthop. Res. Rev.*, vol. 17, no. May, pp. 175–188, 2025, doi:10.2147/ORR.S521832.
[14] P. Aroonjarattham and M. Chanasakulniyom, "Biomechanical Effect of Filled Biomaterials on Distal Thai Femur by Finite Element Analysis," 2015.
[15] B. Dou, F. Zhang, M. Ni, Y. Dai, Z. Wang, and T. Qin, "Biomechanical and finite element study of drilling sites for benign lesions in femoral head and neck with curettage , bone-grafting and internal fixation," vol. 16, no. August, pp. 7808–7828, 2019, doi:10.3934/mbe.2019392.
[16] P. K. Wu, C. W. Lee, W. H. Sun, and C. L. Lin, "Biomechanical analysis and design method for patient-specific reconstructive implants for large bone defects of the distal lateral femur," *Biosensors*, vol. 12, no. 1, 2022, doi:10.3390/bios12010004.
[17] A. Ghouchani, G. Rouhi, and M. H. Ebrahimzadeh, "Post-operative fracture risk assessment following tumor curettage in the distal femur: a hybrid in vitro and in silico biomechanical approach," *Sci. Rep.*, vol. 10, no. 1, pp. 1–13, 2020, doi:10.1038/s41598-020-78188-3.
[18] P. Bazyar, A. Baumgart, H. Altenbach, and A. Usbeck, "An Overview of Selected Material Properties in Finite Element Modeling of the Human Femur," *Biomech.*, vol. 3, no. 1, pp. 124–135, 2023, doi:10.3390/biomechanics3010012.
[19] T. V. Chirila and Y. Hong, *The vitreous humor*. 2016. doi:10.1007/978-1-4939-3305-1_12.
[20] Z. Sheikh, S. Najeeb, Z. Khurshid, V. Verma, H. Rashid, and M. Glogauer, "Biodegradable materials for bone repair and tissue engineering applications," *Materials (Basel).*, vol. 8, no. 9, pp. 5744–5794, 2015, doi:10.3390/ma8095273.
[21] P. Dec, A. Modrzejewski, and A. Pawlik, "Existing and Novel Biomaterials for Bone Tissue Engineering," *Int. J. Mol. Sci.*, vol. 24, no. 1, pp. 1–14, 2023, doi:10.3390/ijms24010529.
[22] I. Ajaxon *et al.*, "Elastic properties and strain-to-crack-initiation of calcium phosphate bone cements: Revelations of a high-resolution measurement technique," *J. Mech. Behav. Biomed. Mater.*, vol. 74, no. June, pp. 428–437, 2017, doi:10.1016/j.jmbbm.2017.06.023.
[23] I. Ayadi and F. Ben Ayed, "Mechanical optimization of the composite biomaterial based on the tricalcium phosphate, titania and magnesium fluoride," *J. Mech. Behav. Biomed. Mater.*, vol. 60, pp. 568–580, 2016, doi:10.1016/j.jmbbm.2016.03.020.
[24] I. Koh, A. López, B. Helgason, and S. J. Ferguson, "The compressive modulus and strength of saturated calcium sulphate dihydrate cements: Implications for testing standards," *J. Mech. Behav. Biomed. Mater.*, vol. 34, pp. 187–198, 2014, doi:10.1016/j.jmbbm.2014.01.018.
[25] L. C. Gerhardt and A. R. Boccaccini, "Bioactive glass and glass-ceramic scaffolds for bone tissue engineering," *Materials (Basel).*, vol. 3, no. 7, pp. 3867–3910, 2010, doi:10.3390/ma3073867.
[26] H. A. Bai *et al.*, "Biomechanical evaluation of three implants for treating unstable femoral intertrochanteric fractures: finite element analysis in axial, bending and torsion loads," *Front. Bioeng. Biotechnol.*, vol. 11, no. November, pp. 1–10, 2023, doi:10.3389/fbioe.2023.1279067.
[27] R. A. Moga, C. D. Olteanu, B. M. Daniel, and S. M. Buru, "Finite Elements Analysis of Tooth — A Comparative Analysis of Multiple Failure Criteria," 2023. doi:0.3390/ijerph20054133.
[28] H. Yang, X. Ma, and T. Guo, "Some factors that affect the comparison between isotropic and orthotropic inhomogeneous finite element material models of femur," *Med. Eng. Phys.*, vol. 32, no. 6, pp. 553–560, 2010, doi:10.1016/j.medengphy.2010.01.004.
[29] A. Gujar, R., Warhatkar, H., & Kale, "Finite element analysis (FEA) of femur to predict biomechanical properties and its validation.," *J. Mech. Eng. Sci.*, vol. 238, no. 5, pp. 1173–1181, 2024, doi:doi:10.1177/09544062231185508.
[30] S. Van Den Munckhof and A. A. Zadpoor, "How accurately can we predict the fracture load of the proximal femur using finite element models?," *Clin. Biomech.*, vol. 29, no. 4, pp. 373–380, 2014, doi: 10.1016/j.clinbiomech.2013.12.018.
[31] Senra, M. R., & Marques, M. d. F. V. (2020). Synthetic Polymeric Materials for Bone Replacement. Journal of Composites Science, 4(4), 191. doi:10.3390/jcs4040191.
[32] S. Dallal, B. Eslami, and S. Tiari, "Recent Advances in PEEK for Biomedical Applications: A Comprehensive Review of Material Properties, Processing, and Additive Manufacturing," *Polymers (Basel).*, vol. 17, no. 14, pp. 1–26, 2025, doi:10.3390/polym17141968.
[33] W. Zhang, "Personalised 3D-printed bioactive peek bone plate scaffold for treating femoral defects," pp. 5060–5072, 2025, doi:10.1039/d4ra07573k.
[34] X. Zhang *et al.*, "Polymer-Ceramic Spiral Structured Scaffolds for Bone Tissue Engineering : Effect of Hydroxyapatite Composition on Human Fetal Osteoblasts," vol. 9, no. 1, pp. 2–11, 2014, doi:10.1371/journal.pone.0085871.
[35] R. Agrawal, A. Kumar, M. K. A. Mohammed, and S. Singh, "Biomaterial types, properties, medical applications, and other factors: a recent review," *J. Zhejiang Univ. Sci. A*, vol. 24, no. 11, pp. 1027–1042, 2023, doi:10.1631/jzus.A2200403.
[36] J.-T. Lee *et al.*, "Optimized 3D-Printed Polylactic Acid/Graphene Oxide Scaffolds for Enhanced Bone Regeneration," *Bioengineering*, vol. 12, no. 11, p. 1192, 2025, doi:10.3390/bioengineering12111192.
[37] X. Yan, Y. Wei, Y. Luo, Z. Wu, Z. Liu, and H. Liao, "Functionalization of 3D printed PLGA-based scaffolds for bone regeneration," *Regen. Ther.*, vol. 30, no. May, pp. 884–899, 2025, doi:10.1016/j.reth.2025.10.003.
[38] R. Álvarez-Chimal, L. Pérez-Sánchez, J. Serrano-Bello, F. C. Vázquez-Vázquez, and M. A. Álvarez-Pérez, "3D printing with polylactic acid (PLA) in bone regeneration using animal models: a systematic review," *AIMS Bioeng.*, vol. 12, no. 4, pp. 453–472, 2025, doi:10.3934/bioeng.2025022.
[39] A. Motameni, A. Z. Alshemary, and Z. Evis, "A review of synthesis methods, properties and use of monetite cements as filler for bone defects," *Ceram. Int.*, vol. 47, no. 10, pp. 13245–13256, 2021, doi:10.1016/j.ceramint.2021.01.240.
[40] J. Benevenia *et al.*, "Supplemental Bone Grafting in Giant Cell Tumor of the Extremity Reduces Nononcologic Complications," *Clin. Orthop. Relat. Res.*, vol. 475, no. 3, pp. 776–783, 2017, doi:10.1007/s11999-016-4755-x.
[41] S. Ramanathan, Y. C. Lin, S. Thirumurugan, C. C. Hu, Y. F. Duann, and R. J. Chung, "Poly(methyl methacrylate) in Orthopedics: Strategies, Challenges, and Prospects in Bone Tissue Engineering," *Polymers (Basel).*, vol. 16, no. 3, 2024, doi:10.3390/polym16030367.
[42] D. Liu, C. Cui, W. Chen, J. Shi, B. Li, and S. Chen, "Biodegradable Cements for Bone Regeneration," *J. Funct. Biomater.*, vol. 14, no. 3, 2023, doi:10.3390/jfb14030134.
[43] F. E. Ranjbar *et al.*, "Kaempferol-loaded bioactive glass-based scaffold for bone tissue engineering: in vitro and in vivo evaluation," *Sci. Rep.*, vol. 13, no. 1, pp. 1–14, 2023, doi:10.1038/s41598-023-39505-8.
[44] M. A. Elnaggar, H. A. Elnoamany, and M. K. Eissa, "Clinical evaluation of 3D PEEK implants for skull bone defects repair: a

single center case serious," *Egypt. J. Neurosurg.*, vol. 40, no. 1, 2025, doi:10.1186/s41984-025-00374-0.

[45] S. Farjaminejad *et al.*, "Advances and Challenges in Polymer-Based Scaffolds for Bone Tissue Engineering: A Path Towards Personalized Regenerative Medicine," *Polymers (Basel).*, vol. 16, no. 23, 2024, doi:10.3390/polym16233303.

[46] R. De Pace, S. Molinari, E. Mazzoni, and G. Perale, "Bone Regeneration : A Review of Current Treatment Strategies," pp. 1–38, 2025. doi:10.3390/jcm14061838.

[47] H. T. Lu, C. C. Hsu, Q. Q. Jian, and W. T. Chen, "Biomechanical Study of Different Scaffold Designs for Reconstructing a Traumatic Distal Femur Defect Using Patient-Specific Computational Modeling," *C. - Comput. Model. Eng. Sci.*, vol. 142, no. 2, pp. 1883–1898, 2025, doi:10.32604/cmes.2025.057675.

[48] W. Chen, X., Tang, T., Chen, T., Li, Q., & Zhang, "Mechanical stability of intertrochanteric fracture of femur with different internal fixation systems," *Chinese J. Tissue Eng. Res.*, vol. 29, no. 9, 2025.

[49] P. A. Motlagh, M. Mirzaei, and V. Naeini, "Failure Prediction of Proximal Femur using quantitative computed tomography based finite element method," vol. 15, no. 5, pp. 153–158, 2025. https://dor.isc.ac/dor/20.1001.1.10275940.1394.15.5.11.5.

[50] A. Type and A. History, "Biomechanical Analysis of Effect of Inclination Angle on Stress Distribution in the Acetabulum and Acetabularcup after Total Hip Arthroplasty," vol. 19, no. 3, pp. 559–567, 2019. https://dor.isc.ac/dor/20.1001.1.10275940.1397.19.3.9.3